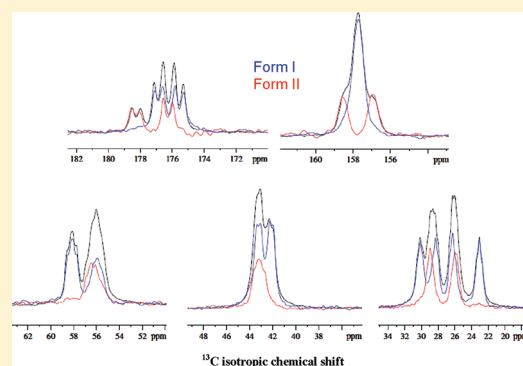


# Disentangling Crystallographic Inequivalence and Crystallographic Forms of L-Arginine by One- and Two-Dimensional Solid-State NMR Spectroscopy

Jose-Enrique Herbert-Pucheta,<sup>†,‡,§</sup> Henri Colaux,<sup>†,‡,§</sup> Geoffrey Bodenhausen,<sup>†,‡,§</sup> and Piotr Tekely<sup>\*,†,‡,§</sup><sup>†</sup>Ecole Normale Supérieure, Département de Chimie, 24 rue Lhomond, 75005 Paris, France<sup>‡</sup>Université Pierre-et-Marie Curie, Place Jussieu, 75005 Paris, France<sup>§</sup>CNRS, UMR 7203, Département de Chimie, 24 rue Lhomond, 75005 Paris, France**S** Supporting Information

**ABSTRACT:** Overlapping  $^{13}\text{C}$  or  $^{15}\text{N}$  solid-state NMR spectra from crystallographically different forms of L-arginine hydrochloride can be separated by exploiting differential proton  $T_1$  relaxation in conjunction with cross-polarization. Dipolar  $^{13}\text{C}$ – $^{13}\text{C}$  and  $^{15}\text{N}$ – $^{15}\text{N}$  two-dimensional correlation experiments reveal resonances belonging to crystallographically and magnetically inequivalent molecules.



## 1. INTRODUCTION

Solid-state NMR can often supplement information obtained from diffraction crystallography.<sup>1</sup> The complementarity of the two techniques is based on the fact that diffraction methods rely on the presence of long-range order, while NMR fingerprints reflect the local environment of the nuclei. Various physical properties of organic and inorganic compounds, including pharmaceutical compounds and synthetic or natural polymers, depend on the form of the crystals. Different conditions of manufacturing, storage, or usage can lead to the interconversion of different forms. A clear identification of the presence of different forms and the determination of their relative concentrations is of prime interest. The ability of solid-state  $^{13}\text{C}$  NMR to reveal structural changes between different crystal forms of organic and pharmaceutical compounds of low molecular mass has been reviewed recently.<sup>2</sup>

L-Arginine plays an important role in structural biology. The guanidinium group of the side chain is positively charged in both acidic and basic environments and may be involved in multiple hydrogen bonds due to the conjugation of its chemical bonds and the delocalization of its positive charge. Arginine is also commonly used in solid-state NMR as a model compound for biological solids to demonstrate the performance of newly developed methods, especially for two-dimensional (2D) homo- and heteronuclear correlation spectroscopy.<sup>3–7</sup>

Single-crystal X-ray studies revealed the existence of two forms of L-arginine hydrochloride: the anhydrous form (L-arginine · HCl)

and the monohydrate (L-arginine · HCl · H<sub>2</sub>O). Both belong to the crystallographic space group  $P2_1$  and have two crystallographically inequivalent molecules per asymmetric unit cell.<sup>8</sup> Although the conformation of the backbone comprising the  $\text{C}'$  and  $\text{C}^\alpha$  carbons is nearly the same in the two forms, the side-group conformations are entirely different, jutting out in two nearly perpendicular directions.<sup>8a</sup>

Companies providing chemicals to research laboratories usually do not specify the crystal form of compounds that can appear in different forms or mixtures thereof. To the best of our knowledge, an unequivocal assignment of solid-state NMR spectra of arginine and the distinction between spectral features arising from different forms and crystallographically inequivalent molecules in the unit cell have not been reported so far. Either one<sup>3</sup> or two<sup>4–6</sup> sets of  $^{13}\text{C}$  resonances have been observed, and the presence of two resonances for each aliphatic carbon was ascribed either to two crystallographically inequivalent molecules in the asymmetric unit cell<sup>4</sup> or to two different crystal forms.<sup>5,6</sup>

In this work, we show how one- and two-dimensional solid-state NMR experiments can help to disentangle spectral features from crystallographic and magnetic inequivalence and different crystallographic forms and allow one to assign unequivocally all

**Received:** October 7, 2011**Revised:** November 15, 2011**Published:** December 07, 2011

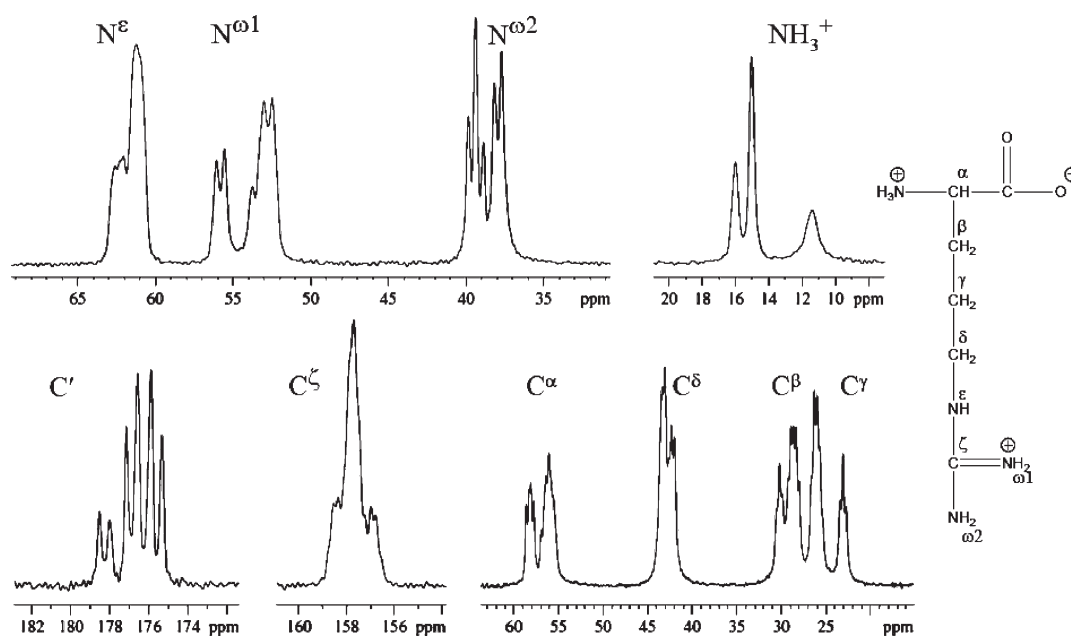


Figure 1. Carbon-13 (bottom) and nitrogen-15 (top) CP/MAS spectra of L-arginine hydrochloride (sample 1).

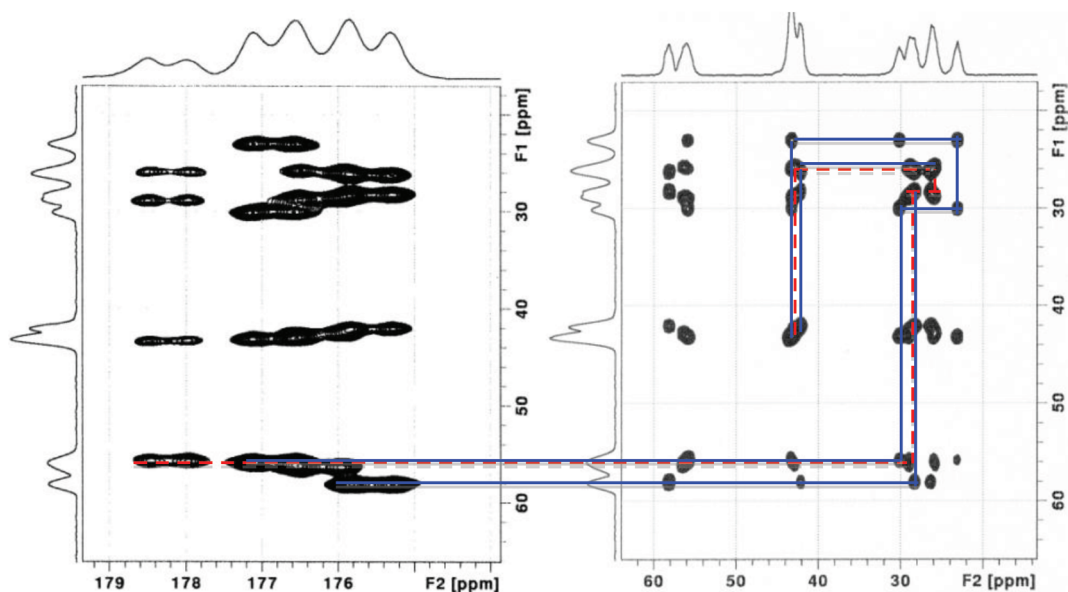


Figure 2. PARIS-xy  $^{13}\text{C}$ – $^{13}\text{C}$  correlation spectrum of L-arginine hydrochloride (sample 1). The spectrum was recorded with a spinning frequency of 27.2 kHz using a proton recoupling  $rf$  amplitude of 15 kHz during 200 ms. Three distinct correlation pathways between directly bound carbons involving one or two resonances for each chemically inequivalent aliphatic carbon are highlighted respectively in red (dashed lines) and blue (continuous lines).

$^{13}\text{C}$  and  $^{15}\text{N}$  resonance lines of a sample of L-arginine hydrochloride that contains a mixture of two crystallographic forms.

## 2. EXPERIMENTAL SECTION

All experiments with fully  $^{13}\text{C}$  and  $^{15}\text{N}$ -labeled L-arginine hydrochloride, purchased from Cambridge Isotope Laboratories (sample 1), fully  $^{13}\text{C}$ ,  $^{15}\text{N}$ -labeled L-arginine hydrochloride monohydrate purchased from Cortecnet (sample 2), and natural abundance anhydrous L-arginine hydrochloride purchased from Sigma Aldrich (sample 3) were performed in a magnetic field of

9.4 T (400 MHz for  $^1\text{H}$ ) using spinning frequencies in the range between 20 and 30 kHz. The  $^{13}\text{C}$  chemical shifts were referenced with respect to the carboxyl carbon of  $\alpha$ -glycine ( $\delta_{\text{iso}} = 176.5$  ppm) used as an external reference,<sup>9</sup> while the  $^{15}\text{N}$  chemical shifts were referenced to  $^{15}\text{NH}_4\text{NO}_3$  ( $\delta_{\text{iso}} = -6.7$  ppm). The recently introduced phase-alternated recoupling irradiation scheme (PARIS)<sup>10</sup> and its phase-shifted counterpart PARIS-xy<sup>11</sup> were used for 2D  $^{15}\text{N}$ – $^{15}\text{N}$  and  $^{13}\text{C}$ – $^{13}\text{C}$  correlation experiments, respectively. Both recoupling methods use an  $rf$  field applied only to the protons with a moderate constant  $rf$  amplitude, using pulse durations equal to half a rotor period  $\tau_p = \tau_{\text{rot}}/2$ . For PARIS irradiation, the

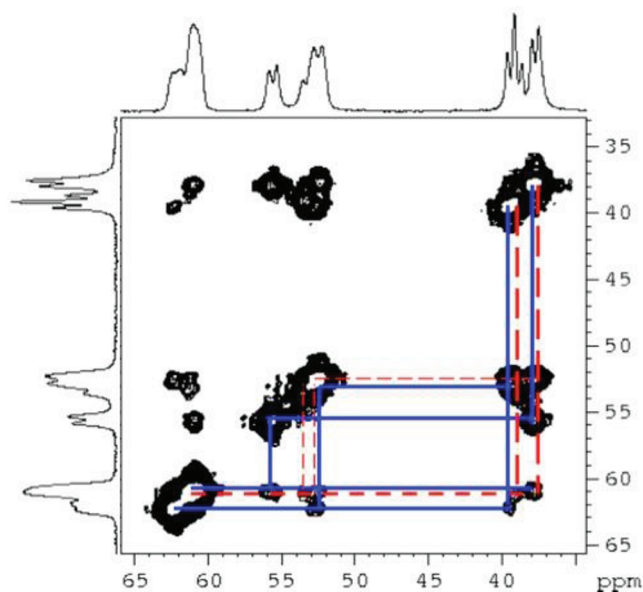


**Figure 3.** PARIS  $^{15}\text{N}$ – $^{15}\text{N}$  correlation spectrum of L-arginine hydrochloride (sample 1). The spectrum was recorded with a spinning frequency of 30 kHz using a proton recoupling  $r_f$  amplitude of 15 kHz during 1 s. The correlations involving the three nitrogen nuclei of the guanidinium group are highlighted in color.

phase is periodically toggled between  $+x$  and  $-x$  after each half of a rotor period. PARIS-xy irradiation also uses pulses with a duration  $\tau_p$  equal to half the rotor period but consists of a block of  $m$  pairs of phase-alternated pulses  $[(x)(-x)]_m$  followed by a phase-shifted block  $[(y)(-y)]_m$  to promote efficient exchange of magnetization between spectrally distant carbons.<sup>11</sup> The  $^1\text{H}$  and  $^{13}\text{C}$   $T_1$  relaxation rates were measured respectively indirectly via  $^{13}\text{C}$ <sup>12</sup> and using the  $T_1\text{CP}$  pulse sequence<sup>13</sup> at 295 K. PISSARRO heteronuclear decoupling<sup>14</sup> was applied during both evolution and detection intervals.

### 3. RESULTS AND DISCUSSION

**3.1. One-Dimensional  $^{13}\text{C}$  and  $^{15}\text{N}$  Spectra.** Figure 1 shows the  $^{13}\text{C}$  (bottom) and  $^{15}\text{N}$  (top) cross-polarization/magic-angle spinning (CP/MAS) spectra of uniformly  $^{13}\text{C}$ ,  $^{15}\text{N}$ -labeled L-arginine hydrochloride (sample 1) recorded with a CP contact time of 1 ms and a spinning frequency  $\nu_{\text{rot}} = 27$  kHz. Both spectra show, besides splittings due to scalar  $J_{\text{C-C}}$  and  $J_{\text{C-N}}$  couplings (see the Supporting Information), two or more resonance signals for each chemically inequivalent nucleus. Interestingly, the relative intensities of the different resonance peaks for each carbon or nitrogen nucleus differ significantly and remain unchanged for different CP contact times, spinning frequencies, and sample temperatures (data not shown). These features are not consistent with the fact that there are only two inequivalent molecules in the asymmetric unit cell. In fact, both spectra strongly suggest the presence of partially overlapping resonance signals from different crystallographic forms with different multiplicities at different sites due to crystallographic and/or magnetic inequivalence. The conformations of the two molecules per asymmetric unit cell of anhydrous L-arginine HCl are not significantly different, in contrast to the case of L-arginine HCl monohydrate that has dihedral angles about the  $\text{C}^\delta\text{--N}^\epsilon$  bond with opposite signs.<sup>8a</sup> This can lead to different multiplicities of magnetically

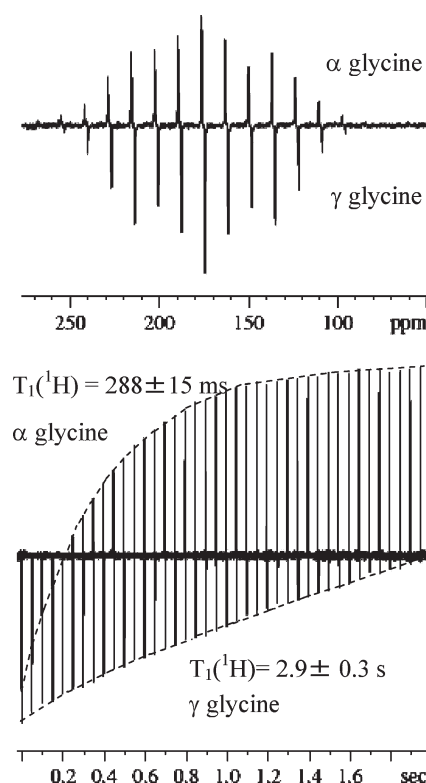


**Figure 4.** (Bottom) Changes in the  $^{13}\text{C}$  signal intensities of carboxyl carbons in  $\alpha$  and  $\gamma$  polymorphs of glycine vs the inversion-recovery time of proton magnetization prior to cross-polarization. The spinning frequency was equal to 27.2 kHz. (Top) Spinning sideband families due to the  $^{13}\text{C}$  CSA's of the carboxyl carbons of the two polymorphs recorded at a spinning frequency of 1.322 kHz using a 500 ms inversion-recovery period of the proton magnetization.

inequivalent sites in different crystallographic forms for chemically equivalent carbons. Regrettably, the relevant resonances of the two forms cannot be easily separated by varying the CP contact time, since the proton  $T_{1\rho}$  relaxation times are not sufficiently differentiated, as is the case of  $\alpha$  and  $\gamma$  polymorphs of L-glycine<sup>9a</sup> for example.

**3.2. Two-Dimensional  $^{13}\text{C}$ – $^{13}\text{C}$  and  $^{15}\text{N}$ – $^{15}\text{N}$  Correlation Experiments.** Two-dimensional homonuclear correlation spectroscopy provides a powerful tool for the determination of spectral connectivities and for the assignment of resonance lines. Efficient magnetization transfer between spins  $S$  such as carbon-13 or nitrogen-15 is a prerequisite for the assignment of solid-state NMR spectra of isotopically enriched molecules in biosolids. Magnetization transfer can be brought about either via through-bond scalar couplings or via through-space dipolar interactions, provided the latter are recoupled to compensate for the effect of magic angle spinning (MAS). Here, we exploit 2D dipolar  $^{13}\text{C}$ – $^{13}\text{C}$  and  $^{15}\text{N}$ – $^{15}\text{N}$  correlation experiments to reveal spectral connectivities and separate sets of highly entangled resonances. As far as we know, 2D correlation spectroscopy has not been used so far to assign resonance signals in samples containing mixtures of different crystallographic forms with inequivalent molecules in asymmetric unit cells. To promote dipolar recoupling, we used both PARIS and PARIS-xy methods to achieve an efficient exchange of magnetization over a large range of spinning frequencies and static magnetic fields.<sup>10,11</sup>

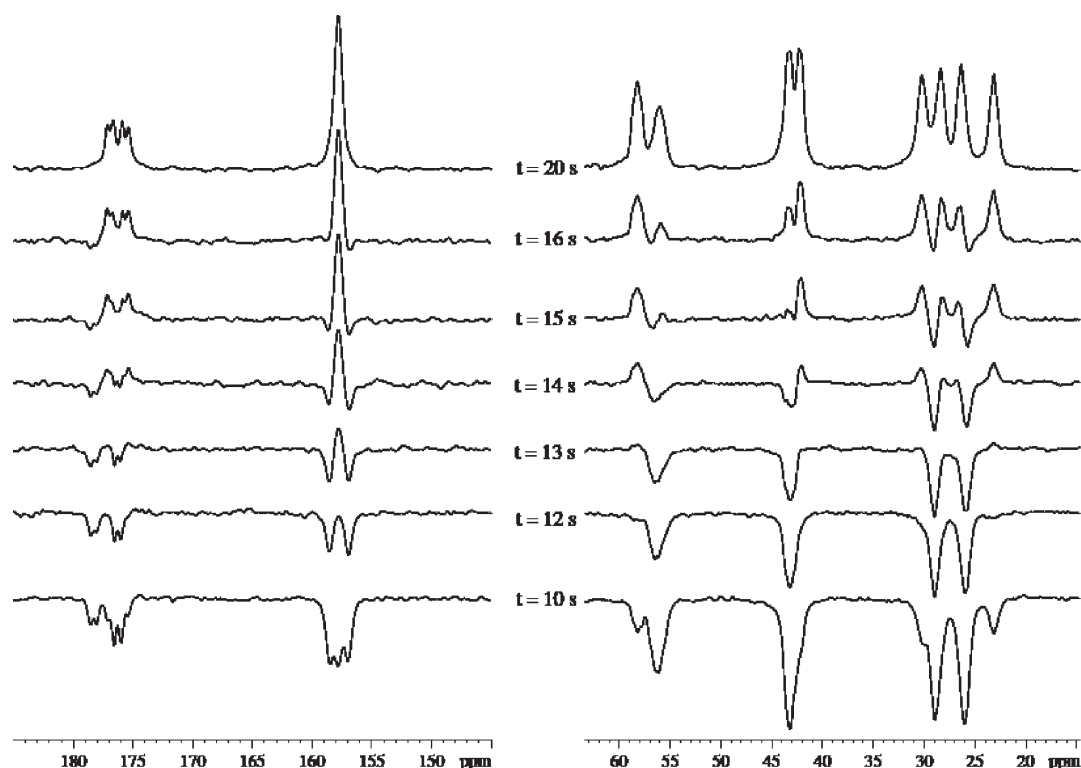


**Figure 5.** Changes in the intensities of the  $^{13}\text{C}$  signals of arginine (sample 1) vs the inversion-recovery time  $10 < t < 20$  s of the proton magnetization preceding cross-polarization. The separation of the spectra of the two forms is best accomplished for proton recovery times  $t = 12$  and  $20$  s. All spectra were recorded at a spinning frequency of  $27.2$  kHz.

**Table 1.** Isotropic Chemical Shifts (in ppm) of  $^{13}\text{C}$  and  $^{15}\text{N}$  of Monohydrate and Anhydrous Forms of L-Arginine Hydrochloride for Two Crystallographically Inequivalent Molecules in the Asymmetric Unit Cell

	$^{13}\text{C}$											
	$\text{C}'$ (1)	$\text{C}'$ (2)	$\text{C}^\alpha$ (1)	$\text{C}^\alpha$ (2)	$\text{C}^\beta$ (1)	$\text{C}^\beta$ (2)	$\text{C}^\gamma$ (1)	$\text{C}^\gamma$ (2)	$\text{C}^\delta$ (1)	$\text{C}^\delta$ (2)	$\text{C}^\xi$ (1)	$\text{C}^\xi$ (2)
L-arginine HCl·H <sub>2</sub> O	176.8	175.5	58.1	56.0	30.1	28.5	26.1	23.0	43.2	42.2	157.7	157.7
L-arginine HCl	178.2	176.2	56.0	56.0	28.6	28.6	26.0	26.0	43.2	43.2	158.4	156.8
	$^{15}\text{N}$											
	$\text{N}^\epsilon$ (1)	$\text{N}^\epsilon$ (2)	$\text{N}^{\omega 1}$ (1)	$\text{N}^{\omega 1}$ (2)	$\text{N}^{\omega 2}$ (1)	$\text{N}^{\omega 2}$ (2)	$\text{NH}_3$ (1)	$\text{NH}_3$ (2)				
L-arginine HCl·H <sub>2</sub> O	62.2	61.0	53.5	52.5	39.1	37.7	15.0	11.2				
L-arginine HCl	61.0	61.0	55.6	52.5	39.0	38.0	15.4	15.4				

Figure 2 shows extracts of a 2D  $^{13}\text{C}$ – $^{13}\text{C}$  correlation spectrum of sample 1 recorded at  $\nu_{\text{rot}} = 27.2$  kHz with PARIS-xy ( $m = 1$ ) recoupling with an  $rf$  amplitude  $\nu_{1\text{H}} = 15$  kHz during  $\tau_m = 200$  ms. Despite the relatively high spinning frequency and modest  $rf$  recoupling amplitude, the spectrum provides unequivocal evidence of the broad bandwidth of recoupling achieved by the PARIS-xy scheme, which can induce magnetization exchange simultaneously between nearby aliphatic carbons and between spectrally distant  $\text{C}'$  or  $\text{C}^\xi$  and aliphatic signals (see the Supporting Information). Note that all correlations (up to four bonds) clearly appear, permitting one to disentangle unequivocally all spectrally correlated resonances. Somewhat unexpectedly, each aliphatic subset correlates with two out of four carboxyl resonances, one of them overlapping with two others (Figure 2, left).

Equally interestingly, two resonance signals of the  $\text{C}^\delta$  carbon correlate with a central  $\text{C}^\xi$  resonance line while the third subset involving  $\text{C}^\delta$  correlates with two remaining resonances of the  $\text{C}^\xi$  carbon (see the Supporting Information). This reveals that two crystallographically inequivalent molecules in the unit cell may lead to either one or two distinct isotropic chemical shifts for each (chemically inequivalent) carbon. Indeed, some sites can have identical (or very similar) isotropic chemical shifts, even if their anisotropic chemical shift tensors are different in orientation and/or magnitude.<sup>15</sup> Such situations are quite common in solids for symmetry-related sites (crystallographic sites that are related by mirror-plane symmetry or by two- or higher-fold axes of symmetry). These congruent sites should be distinguished from magnetically equivalent sites for which the chemical shift

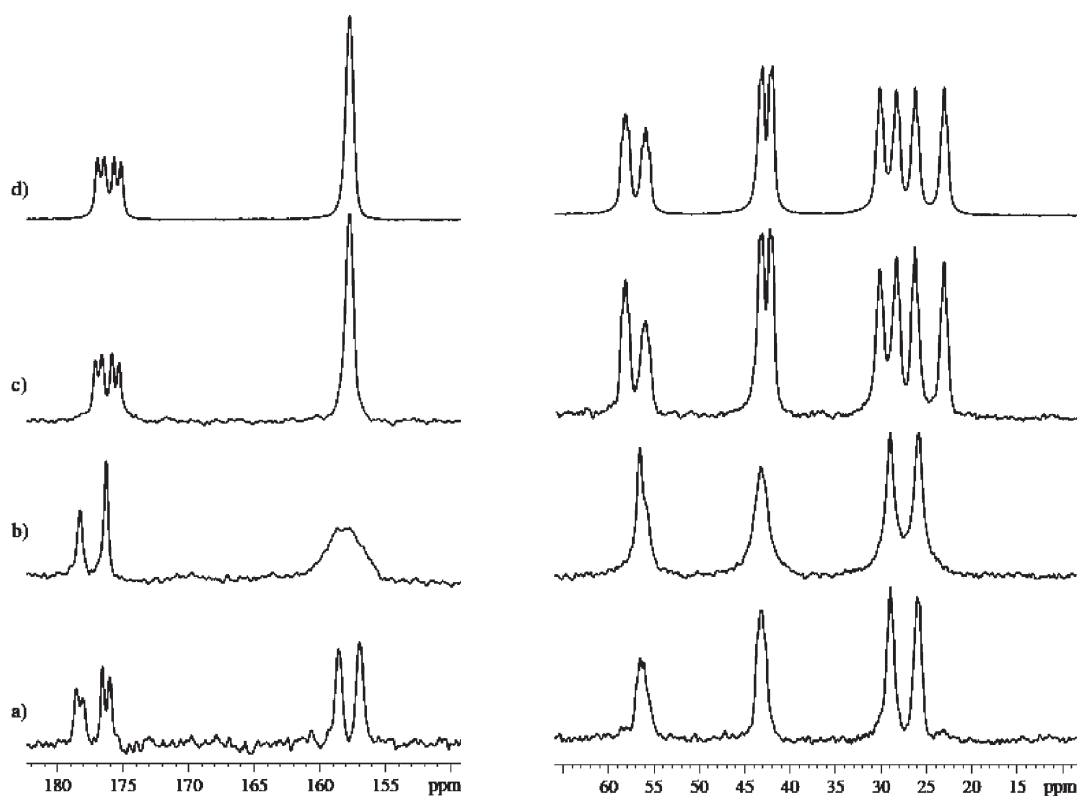


**Figure 6.** (a) High- and low-frequency regions of a  $T_1(^1\text{H})$  relaxation-edited  $^{13}\text{C}$  CP/MAS spectrum of uniformly  $^{13}\text{C}$ ,  $^{15}\text{N}$  labeled L-arginine HCl (sample 1) recorded with a proton inversion-recovery delay  $t = 12$  s. (b) Natural abundance  $^{13}\text{C}$  CP/MAS spectrum of anhydrous L-arginine HCl (sample 3). Note the broadening of the  $\text{C}^\alpha$  resonance due to residual dipolar couplings to the three neighboring  $^{14}\text{N}$  nuclei. (c) Proton  $T_1(^1\text{H})$  edited  $^{13}\text{C}$  CP/MAS spectrum of sample 1 recorded with an inversion-recovery delay  $t = 20$  s. (d)  $^{13}\text{C}$  CP/MAS spectrum of uniformly  $^{13}\text{C}$ ,  $^{15}\text{N}$  labeled L-arginine HCl  $\cdot$  H $_2$ O (sample 2).

tensors are identical both in magnitude and orientation, which occurs for crystallographic sites that are related either by inversion symmetry or by translation.<sup>15</sup> In all remaining cases, both the isotropic and, in general, the anisotropic components of the chemical shift tensors are different.

In spite of these ambiguous features, the  $^{13}\text{C}$ – $^{13}\text{C}$  correlation spectrum in Figure 2 clearly reveals the presence of three distinct sets of resonances (single-bond correlation pathways involving one and two resonances for each chemically inequivalent aliphatic carbon are highlighted in red and blue, respectively). However, a clear distinction of the relevant resonances is less evident in the 2D  $^{15}\text{N}$ – $^{15}\text{N}$  correlation spectrum of Figure 3, in spite of efficient magnetization exchange between the three nitrogen sites of the guanidinium group. In fact, although roughly four sets of correlations can be identified in Figure 3, unambiguous pathways are hardly discernible due to resonance overlaps. The 2D dipolar  $^{13}\text{C}$ – $^{15}\text{N}$  correlation spectra (see the Supporting Information) do not come to our rescue for the same reason. This prompted us to attempt spectral editing of relevant forms by exploiting differences in their relaxation properties.

**3.3. Editing of  $^{13}\text{C}$  and  $^{15}\text{N}$  Spectra from Different Crystallographic Forms through  $^1\text{H}$  Spin-Lattice Relaxation.** Distinct  $T_{1\rho}$  or  $T_1$  proton relaxation times associated with different crystallographic forms or polymorphs of a given compound may originate from multiple sources.<sup>9a,16,17</sup> First, differences in crystal hydration, besides effects on hydrogen-bond networks, can lead to changes in spectral densities of libration modes in the mid-kilohertz and/or megahertz frequency ranges. Another reason for different proton relaxation rates in different crystallographic

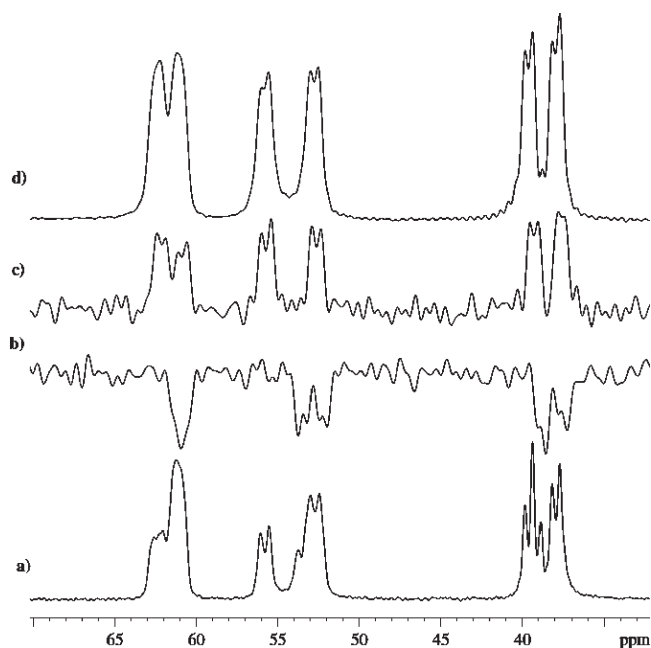


**Figure 7.** (a)  $^{15}\text{N}$  CP/MAS spectrum of L-arginine HCl (sample 1). The spectra of the two crystallographic forms are best separated by using different inversion-recovery times of the proton magnetization preceding the cross-polarization transfer  $t = 12$  s (b) and 20 s (c). (d)  $^{15}\text{N}$  CP/MAS spectrum of L-arginine HCl  $\cdot$  H $_2$ O (sample 2). No apodization function was applied. The spectra (a–d) were recorded with 800, 256, 256, and 1024 scans, respectively.



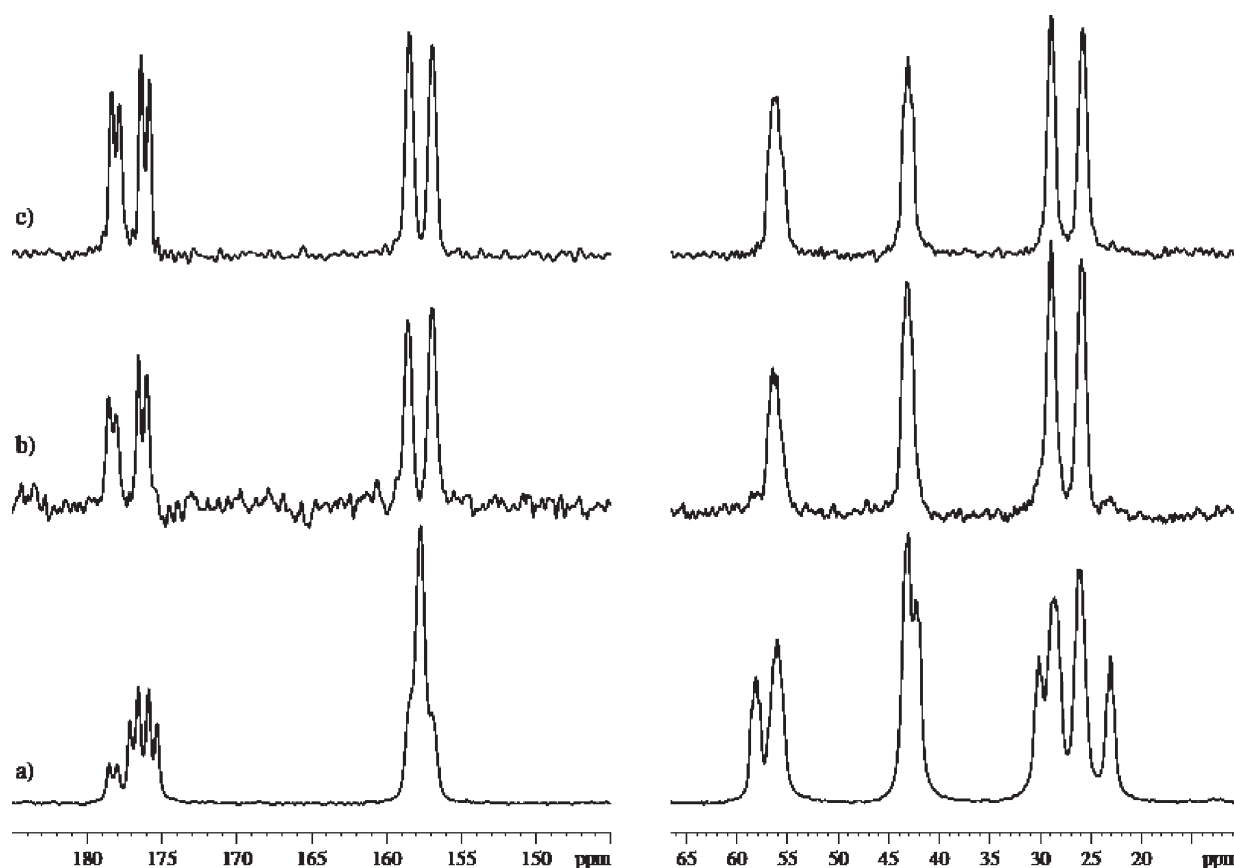


**Figure 8.** (a)  $^{13}\text{C}$  CP/MAS spectrum of L-arginine HCl (sample 1). The separate spectra of the slowly relaxing form were recorded (b) with a proton relaxation delay  $t = 12$  s and (c) with a  $^{13}\text{C}$  relaxation delay  $t = 150$  s (see Figure 5).

forms and polymorphs may arise from different rates of reorientation of  $\text{CH}_3$  and  $\text{NH}_3^+$  groups. Thus, the proton  $T_1$  relaxation times of ammonium groups have been found to be significantly different for  $\alpha$  and  $\gamma$  glycine.<sup>16</sup> These two polymorphs exhibit different energy barriers for the  $\text{NH}_3^+$  rotation due to differences in hydrogen bonds.<sup>16</sup> In rigid and strongly dipolar-coupled solids, the overall proton spin-lattice relaxation rates are averaged by spin diffusion that leads to a uniform relaxation rate of all protons in the spin system, except for protons belonging to rapidly rotating methyl and ammonium  $\text{NH}_3^+$  groups that can play a role of magnetization ‘sinks’. As illustrated in Figure 4, taking advantage of different proton  $T_1$  relaxation times ( $T_1(^1\text{H}) = 0.29$  and  $2.9$  s for  $\alpha$  and  $\gamma$  glycine, respectively) combined with  $^1\text{H} \rightarrow ^{13}\text{C}$  cross-polarization, allows one to record  $^{13}\text{C}$  spectra of glycine where the resonance signals of carboxyl groups that belong to different polymorphs have opposite phases.

Rapidly rotating  $\text{NH}_3^+$  groups may play a role of a magnetization ‘sink’ in arginine. The packing of the arginine molecules in both forms is determined by a three-dimensional network of hydrogen bonds, with as many as five hydrogen bonds involving each guanidyl group.<sup>8a</sup> In the case of L-arginine HCl monohydrate, all 20 hydrogen atoms in the asymmetric unit cell that are bound to nitrogen and oxygen are involved in such bonds.<sup>8c</sup> This extensive system of hydrogen bonds and the high-frequency librations of the water molecules are expected to affect the proton spin-lattice relaxation rates.

To prove this hypothesis, we exploited, as for the  $\alpha$  and  $\gamma$  polymorphs of glycine (Figure 4), the combination of cross-polarization

and proton spin-lattice relaxation. As shown in Figure 5, after inversion of the proton magnetization followed by partial recovery during 12 s, a number of resonance signals simultaneously vanish in the  $^{13}\text{C}$  CP/MAS spectrum of sample 1, due to the zero-passage of the fastest-relaxing component. The remaining negative resonance lines all vanish in turn after a recovery time of 20 s. Assuming monoexponential relaxation in each crystallographic form, these two recovery delays correspond roughly to proton relaxation times  $T_1(^1\text{H}) = 17.3$  and  $28.8$  s, respectively.

Besides the two distinct pairs of carboxyl resonances, the spectra recorded with proton inversion-recovery times of 12 and 20 s show a number of striking differences, that is, one or two resonance signals for each aliphatic and  $\text{C}^\zeta$  carbon in the first spectrum and two or one resonance lines for each aliphatic and  $\text{C}^\zeta$  carbon in the second spectrum (see Table 1). These two distinct sets of resonances fully corroborate the correlations revealed by two-dimensional exchange experiments (Figure 2) and indeed correspond to separate  $^{13}\text{C}$  spectra of the two crystallographic forms, as independently checked by recording the  $^{13}\text{C}$  CP/MAS spectra of samples 2 and 3 that contain unique pure forms (Figure 6, also see the Supporting Information).

One can obviously exploit the differential recovery rates of the proton magnetization for the purpose of editing the strongly overlapping  $^{15}\text{N}$  CP/MAS spectra of the crystallographically different forms. This is shown in Figure 7 where the individual  $^{15}\text{N}$  spectra of each form were recorded with the same recovery delays that allowed editing of the  $^{13}\text{C}$  spectra, thus corroborating again the spectral connectivities of Figure 3 (highlighted in red

and blue within individual forms). This proves that, in analogy to the proton  $T_1$  (Figure 4) and  $T_{1\rho}$  relaxation times in  $\alpha$  and  $\gamma$  polymorphs of glycine,<sup>9a</sup> the  $T_1(^1\text{H})$  relaxation in arginine can be successfully exploited to disentangle overlapping  $^{13}\text{C}$  or  $^{15}\text{N}$  spectra from two crystallographically different forms that coexist in a powder sample.

Efficient spin diffusion in strongly dipolar-coupled proton systems is also likely to affect the longitudinal relaxation times  $T_1(S)$  of low gamma nuclei  $S = ^{13}\text{C}$ ,  $^{15}\text{N}$ , and so forth, which could differ in crystallographically different forms in analogy to the proton  $T_1$  relaxation times  $T_1(^1\text{H})$ . For example, the  $T_1(^{13}\text{C})$  relaxation times of carboxyl carbons in  $\alpha$ -glycine have been observed to be five times shorter than in  $\gamma$ -glycine.<sup>9a</sup> Longitudinal  $T_1(^{13}\text{C})$  relaxation measurements on sample 1 reveal a biexponential decay of the magnetization for all types of carbons (see the Supporting Information). The difference in the  $^{13}\text{C}$  spin-lattice relaxation rates may be exploited to record the fully separated spectrum of the slowly relaxing form, as shown in Figure 8, although this approach is significantly more time-consuming. Because of the much slower spin-lattice relaxation of  $^{15}\text{N}$ , this approach to spectral editing is hardly applicable to these nuclei. As demonstrated elsewhere, selective excitation and equilibration of magnetization within a given crystallographic form or polymorph may be used for the separation of spectral fingerprints associated with individual forms or polymorphs in slowly relaxing spin systems when the required difference in relaxation rates turns out to be insufficient for editing purposes.<sup>18</sup>

#### 4. CONCLUSIONS

We have demonstrated that the combination of one- and two-dimensional solid-state NMR experiments makes it possible to disentangle overlapping spectral fingerprints due to the presence of two different crystallographic forms and to two crystallographically inequivalent sites in each unit cell in L-arginine hydrochloride. This leads to an unequivocal assignment of all  $^{13}\text{C}$  and  $^{15}\text{N}$  resonance lines of the two different forms, each of which is endowed with two crystallographically inequivalent molecules per asymmetric unit cell. The approach presented in this work should be useful for spectral editing of a broad range of polymorphic and multicomponent systems, including pharmaceutical compounds, polymer materials, microcrystalline proteins, and Alzheimer  $\beta$ -amyloid fibrils.

#### ■ ASSOCIATED CONTENT

Supporting Information.  $^{13}\text{C}$  and  $^{15}\text{N}$  CP/MAS spectra with expansions of the  $J$ -splitting patterns, 2D  $^{13}\text{C}$ – $^{13}\text{C}$  and  $^{13}\text{C}$ – $^{15}\text{N}$  correlation spectra, and  $T_1(^{13}\text{C})$  relaxation data. This material is available free of charge via the Internet at <http://pubs.acs.org>.

#### ■ AUTHOR INFORMATION

##### Corresponding Author

\*E-mail: [Piotr.Tekely@ens.fr](mailto:Piotr.Tekely@ens.fr).

#### ■ ACKNOWLEDGMENT

Financial support from the Agence Nationale de la Recherche (project 'FastSpinProts' ANR-09-BLAN-0111-01) and of the CNRS (UMR 7203) is gratefully acknowledged.

#### ■ REFERENCES

- (1) *NMR Crystallography*; Harris, R. K., Wasylishen, R. E., Duer, M. J., Eds.; J. Wiley & Sons Ltd: New York, 2009.
- (2) (a) Harris, R. K. *Analyst* **2006**, *131*, 351. (b) Harris, R. K. *J. Pharm. Pharmacol.* **2007**, *59*, 225.
- (3) Sun, B. Q.; Costa, P. R.; Griffin, R. G. *J. Magn. Reson. A* **1995**, *112*, 191.
- (4) Straus, S. K.; Bremi, T.; Ernst, R. R. *Chem. Phys. Lett.* **1996**, *262*, 709.
- (5) Baldus, M.; Meier, B. H. *J. Magn. Reson. A* **1996**, *121*, 65.
- (6) Leppert, J.; Ohlenschläger, O.; Görlach, M.; Ramachandran, R. *J. Biomol. NMR* **2004**, *29*, 167.
- (7) Duma, L.; Abergel, D.; Ferrage, F.; Pelulessy, P.; Tekely, P.; Bodenhausen, G. *ChemPhysChem* **2008**, *9*, 1104.
- (8) (a) Ramachandran, G. N.; Mazumdar, S. K.; Venkatesan, K.; Lakshminarayanan, A. V. *J. Mol. Biol.* **1966**, *15*, 232. (b) Mazumdar, S. K.; Venkatesan, K.; Lez, H. C.; Donohue, J. Z. *Kristallogr.* **1969**, *130*, 328. (c) Dow, J.; Jensen, L. H.; Mazumdar, S. K.; Srinivasan, R.; Ramachandran, G. N. *Acta Crystallogr.* **1970**, *B26*, 1662.
- (9) (a) Potrzebowski, M. J.; Tekely, P.; Dusaosoy, Y. *Solid State Nucl. Magn. Reson.* **1998**, *11*, 253. (b) Gardiennet, C.; Tekely, P. *Conc. Magn. Reson. A* **2004**, *22*, 106.
- (10) (a) Weingarth, M.; Demco, D. E.; Bodenhausen, G.; Tekely, P. *Chem. Phys. Lett.* **2009**, *469*, 342. (b) Weingarth, M.; Bodenhausen, G.; Tekely, P. *J. Am. Chem. Soc.* **2009**, *131*, 13937.
- (11) (a) Weingarth, M.; Bodenhausen, G.; Tekely, P. *Chem. Phys. Lett.* **2010**, *488*, 10. (b) Weingarth, M.; Masuda, Y.; Takegoshi, K.; Bodenhausen, G.; Tekely, P. *J. Biomol. NMR* **2011**, *50*, 129.
- (12) Tekely, P.; Vignon, M. R. *J. Polym. Sci., Part C: Polym. Lett.* **1987**, *25*, 257.
- (13) Torchia, D. A. *J. Magn. Reson.* **1978**, *30*, 613.
- (14) (a) Weingarth, M.; Tekely, P.; Bodenhausen, G. *Chem. Phys. Lett.* **2008**, *466*, 247. (b) Weingarth, M.; Bodenhausen, G.; Tekely, P. *J. Magn. Reson.* **2009**, *199*, 238. (c) Weingarth, M.; Bodenhausen, G.; Tekely, P. *Chem. Phys. Lett.* **2011**, *502*, 259.
- (15) (a) Tekely, P.; Reichert, D.; Zimmermann, H.; Luz, Z. *J. Magn. Reson.* **2000**, *145*, 173. (b) Tekely, P.; Gardiennet, C.; Potrzebowski, M.; Sebald, A.; Reichert, D.; Luz, Z. *J. Chem. Phys.* **2002**, *116*, 7607. (c) Luz, Z.; Tekely, P.; Reichert, D. *Prog. NMR Spectrosc.* **2002**, *41*, 83.
- (16) Gu, Z.; Ebisawa, K.; McDermott, A. *Solid State Nucl. Magn. Reson.* **1996**, *7*, 161.
- (17) Zumbulyadis, N.; Antalek, B.; Windig, W.; Scaringe, R. P.; Lanzafame, A. M.; Blanton, T.; Helber, M. *J. Am. Chem. Soc.* **1999**, *121*, 11554.
- (18) (a) Hucher, C.; Beaume, F.; Eustache, R. P.; Tekely, P. *Macromolecules* **2005**, *38*, 1789. (b) Tekely, P.; Brondeau, J.; Elbayed, K.; Retournard, A.; Canet, D. *J. Magn. Reson.* **1988**, *80*, 509.